Mineralogical Magazine, June 2012, Vol. 76(3), pp. 743–750

Debattistiite, $Ag_9Hg_{0.5}As_6S_{12}Te_2$, a new Te-bearing sulfosalt from Lengenbach quarry, Binn valley, Switzerland: description and crystal structure

A. Guastoni[1], L. Bindi[2,3] and F. Nestola[4,*]

[1] Museo di Mineralogia, Università degli Studi di Padova, Palazzo Cavalli, Via Matteotti 30, I-35121, Padova, Italy
[2] Dipartimento di Scienze della Terra, Università degli Studi di Firenze, Via G. La Pira 4, I-50121 Firenze, Italy
[3] CNR – Istituto di Geoscienze e Georisorse, Sezione di Firenze, Via G. La Pira 4, I-50121 Firenze, Italy
[4] Dipartimento di Geoscienze, Università degli Studi di Padova, Via Gradenigo 6, I-35131 Padova, Italy

[*Received 13 March 2012; Accepted 2 May 2012; Associate Editor: Giancarlo Della Ventura*]

ABSTRACT

Debattistiite, ideally $Ag_9Hg_{0.5}As_6S_{12}Te_2$, is a new mineral (IMA-CNMNC 2011-098) from the Lengenbach quarry in the Binn Valley, Valais, Switzerland. It occurs as very rare tabular euhedral crystals up to 150 μm across in cavities in dolomitic marble, associated with realgar, rutile, trechmannite and hutchinsonite. Debattistiite is opaque with a metallic lustre and a grey streak. It is brittle; the Vickers hardness (VHN_{25}) is 80 kg mm^{-2} (range: 65–94), corresponding to a Mohs hardness of 2–2½. In reflected light debattistiite is dark grey, highly bireflectant and weakly pleochroic from dark grey to a slightly greenish grey. Between crossed polars it is highly anisotropic with brownish to blue rotation tints. Internal reflections are absent. Reflectance percentages for the four COM wavelengths (R_{min} and R_{max}) are 27.2, 34.5 (471.1 nm), 25.5, 31.0 (548.3 nm), 22.9, 28.4 (586.6 nm), and 20.1, 25.2 (652.3 nm), respectively.

Debattistiite is triclinic, space group $P\bar{1}$, with a = 7.832(5), b = 8.606(4), c = 10.755(5) Å, α = 95.563(9), β = 95.880(5), γ = 116.79(4)°, V = 635.3(6) $Å^3$ and Z = 1. The crystal structure [R_1 = 0.0826 for 795 reflections with $I > 2\sigma(I)$] consists of corner-sharing AsS_3 pyramids forming three-membered distorted rings linked by Ag atoms in triangular or tetrahedral coordination.

The five strongest powder-diffraction lines [d in Å (I/I_0) (hkl)] are as follows: 10.56 (6) (001); 3.301 (5) ($\bar{2}12$); 2.991 (4) ($2\bar{1}2$); 2.742 ($\bar{2}\bar{1}1$) and 2.733 (10) ($\bar{2}30$). A mean of nine electron microprobe analyses gave: Ag 44.88, Hg 4.49, As 20.77, S 17.72, Te 11.82; total 99.68 wt.%, which corresponds to $Ag_{9.02}Hg_{0.49}As_{6.012}S_{11.98}Te_{2.01}$, on the basis of 29.5 atoms. The new mineral is named for Luca De Battisti, a systematic mineralogist and expert on the minerals of Lengenbach quarry.

Keywords: debattistiite, new mineral, sulfosalts, tellurium, Lengenbach, Switzerland.

Introduction

Lengenbach quarry in the Binn Valley, Valais, is one of the most famous mineral localities in Switerland and is well known for rare Pb-Cu-Ag-As-Tl bearing sulfosalts. It is the type locality for the rare thallium-bearing sulfosalts dalnegroite, edenharterite, erniggliite, gabrielite, hatchite, hutchinsonite, imhofite, jentschite, rathite, sartorite, sicherite, stalderite and wallisite (Hofmann *et al.*, 1993; Graeser *et al.*, 2008; Nestola *et al.*, 2010; Bindi *et al.*, 2011). Tellurium-bearing minerals are very rare at the quarry. The presence of tellurium was noted by Graeser *et al.* (2008). Tellurium-rich canfieldite

* E-mail: fabrizio.nestola@unipd.it
DOI: 10.1180/minmag.2012.076.3.21

was subsequently reported by Bindi *et al.* (2012). Debattistiite is the second tellurium-bearing sulfosalt from Lengenbach.

Debattistiite has been identified in two specimens which were found in zone 1 of the quarry in 1996 (Greaser *et al.*, 2008). It occurs with realgar, rutile, trechmannite and hutchinsonite in dolomitic marble. Debattistiite was approved as a new mineral by the IMA Commission (IMA 2011-098). The mineral name honours Luca De Battisti (b. 1958), a systematic mineralogist and expert on Lengenbach minerals. He discovered the new mineral dalnegroite (Nestola *et al.*, 2010) in 2009 and also collected the specimens of debattistiite. He has published several descriptive articles on minerals and new finds from this famous locality (e.g. Guastoni and De Battisti, 2006). Holotype material is deposited in the mineralogical collections of the Museum of Mineralogy of the Department of Geosciences at the University of Padova, Italy, under catalogue number MMP M10680. To our knowledge, debattistiite has no synthetic analogues.

Physical and optical properties

Debattistiite occurs as very rare euhedral tabular crystals, up to 150 μm in size, in cavities in dolomitic marble (Fig. 1). The crystals resemble wallisite and are closely associated with realgar, rutile, trechmannite and hutchinsonite. Debattistiite is black with a grey streak. It is opaque in transmitted light and has a metallic lustre. No cleavage was observed and the fracture is uneven. The calculated density using the empirical formula (see below) is 5.647 g cm^{-3}.

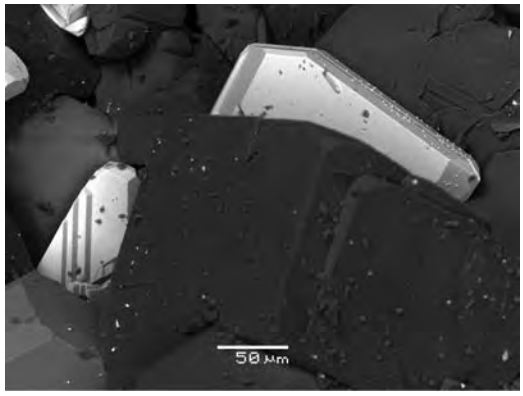

FIG. 1. A backscattered-electron image of debattistiite crystals (bright) in dolomite matrix.

The density could not be measured because of the small grain size. Micro-indentation measurements carried out with a Vickers microhardness tester using a load of 25 g gave a mean value of 80 kg mm^{-2} (range: 65–94) corresponding to a Mohs hardness of 2–2½.

In plane-polarized incident light, debattistiite is dark grey, highly bireflectant and weakly pleochroic varying from dark grey to slightly greenish grey. Between crossed polars, debattistiite is highly anisotropic, with brownish to blue rotation tints. Internal reflections are absent and there is no optical evidence of growth zonation.

Reflectance measurements were performed in air using a Zeiss MPM-200 microphotometer equipped with an MSP-20 system processor on a Zeiss Axioplan ore microscope. The filament temperature was approximately 3350 K. An interference filter was adjusted to select four wavelengths for measurement (471.1, 548.3, 586.6 and 652.3 nm). Readings were taken from the specimen and an SiC calibration standard in the same conditions. The diameter of the measurement spot was 0.1 mm. Reflectance percentages, R_{min} and R_{max}, are 27.2, 34.5 (471.1 nm), 25.5, 31.0 (548.3 nm), 22.9, 28.4 (586.6 nm) and 20.1, 25.2 (652.3 nm), respectively.

X-ray crystallography and crystal structure determination

A crystal fragment (70 × 50 × 40 μm) was selected for an X-ray single-crystal diffraction study which was carried out on a STOE-STADI IV CCD single-crystal diffractometer (Table 1). No systematic absences were observed in the collected data set, leading to the choice of space groups $P1$ and $P\bar{1}$. Statistical tests on the distribution of $|E|$ values ($|E^2-1|$ = 0.965) indicated the presence of an inversion centre, suggesting space group $P\bar{1}$. The positions of the heavy atoms were determined by the charge-flipping method (Oszlányi and Süto, 2008) using the *JANA2006* software package (Petříček *et al.*, 2006). A least-squares refinement on F^2 using these heavy-atom positions and isotropic temperature factors produced an R factor of 0.184. Three-dimensional difference-Fourier syntheses yielded the position of the remaining S atoms. The *JANA2006* program (Petříček *et al.*, 2006) was used to refine the structure.

Of the seven anion positions, one was found to be almost fully occupied by Te [$Te_{0.93(1)}S_{0.07}$]. It is important to note that the Ag4 and Hg

TABLE 1. Crystallographic data and refinement parameters for debattistiite.

Crystal data	
Ideal formula	$Ag_9Hg_{0.5}As_3S_{12}Te_2$
Crystal system	triclinic
Space group	$P\bar{1}$
Unit-cell parameters (Å, º)	7.832(5) 8.606(4) 10.755(5) 95.563(9) 95.880(5) 116.79(4)
Unit-cell volume (Å^3)	635.3(6)
Z	1
Crystal size (mm)	$0.070 \times 0.050 \times 0.040$
Data collection	
Diffractometer	STOE-STADI IV CCD
Temperature (K)	298(3)
Radiation, wavelength (Å)	Mo$K\alpha$, 0.71073
2θ max for data collection (º)	86.18
Crystal-detector distance (mm)	50
h, k, l ranges	$-12 \rightarrow 12$, $-7 \rightarrow 16$, $-16 \rightarrow 20$
Axis, frames, width (º), time per frame (s)	ω–φ, 1380, 1.00, 25
Total reflections collected	8404
Unique reflections (R_{int})	5635 (0.125)
Unique reflections $I > 2\sigma(I)$	795
Data completeness to θ_{max} (%)	99.2
Absorption correction method	*X-RED* and *X-SHAPE*
Structure refinement	
Refinement method	Full-matrix least-squares on I
Data/restraints/parameters	795/0/133
R_1 [$I > 2\sigma(I)$], wR_2 [$I > 2\sigma(I)$]	0.0826, 0.1733
R_1 all, wR_2 all	0.1012, 0.2104
Goodness-of-fit on F^2	0.700
Largest diff. peak and hole (e$^-$ Å^{-3})	3.05, −4.99

$R_{int} = (n/n - 1)^{1/2}[F_o^2 - F_o\,(\text{mean})^2]/\Sigma F_o^2$
$R_1 = \Sigma||F_o| - |F_c||/\Sigma|F_o|$; $wR_2 = \{\Sigma[w(F_o^2 - F_c^2)^2]/\Sigma[w(F_o^2)^2]\}^{1/2}$;
* $w = 1/[\sigma^2(F_o^2) + (aP)^2 + bP]$, where $P = (\max(F_o^2,0) + 2F_c^2)/3$;
$\text{GooF} = \{\Sigma[w(F_o^2 - F_c^2)^2]/(n - p)\}^{1/2}$
where n is the number of reflections and p is the number of refined parameters.

positions, which are very close (separation 1.137 Å), are only partially (50%) occupied (Table 2). The occupancy of these sites was allowed to vary and they were found to be 50% occupied (the analytical uncertainty of the occupancy values is 0.02). After this had been determined, the occupancy of these sites was fixed at 50% in the structure refinement. There is, therefore, a statistical distribution between them (see below). Neutral scattering curves for Ag, Hg, As, S and Te were taken from the *International Tables for X-ray Crystallography* (Ibers and Hamilton, 1974). At the last stage of the refinement, with anisotropic atomic displacement parameters for all atoms and no constraints, the refinement converged at R_1 = 0.0826 for 795 observed reflections (2σ(I) level) and 133 parameters, and at R_1 = 0.1012 for all 5623 independent reflections. The relatively small size of the crystal and its poor quality accounts for the significant difference between the total number of unique reflections measured and those having $I > 2\sigma(I)$.

Inspection of the difference-Fourier map revealed maximum positive and negative peaks of 3.05 and −4.99 e$^-$ Å^{-3}, respectively. Experimental details and R indices are listed in Table 1. Fractional atom coordinates and isotropic

TABLE 2. Atoms, Wyckoff symbol, site occupancy, fractional atom coordinates (Å) and isotropic atomic displacement parameters (Å^2) for debattistiite.

Atom	Wyckoff	Site occupancy	*x*/*a*	*y*/*b*	*z*/*c*	U_{eq}
Ag1	2*i*	$Ag_{1.00}$	−0.0372(4)	0.5057(3)	0.3695(3)	0.0453(9)
Ag2	2*i*	$Ag_{1.00}$	0.5761(4)	0.9562(4)	0.3442(3)	0.060(1)
Ag3	2*i*	$Ag_{1.00}$	0.2110(4)	0.6290(3)	0.1574(4)	0.067(1)
Ag4	2*i*	$Ag_{0.50}$	0.5814(6)	0.5688(5)	0.6241(4)	0.019(1)
Hg4	1*h*	$Hg_{0.50}$	½	½	½	0.024(2)
Ag5	2*i*	$Ag_{1.00}$	0.5248(4)	0.2238(4)	0.1972(4)	0.079(1)
As1	2*i*	$As_{1.00}$	0.1403(4)	0.9740(4)	0.3703(3)	0.0205(8)
As2	2*i*	$As_{1.00}$	−0.2694(4)	0.6768(4)	0.1302(3)	0.0237(8)
As3	2*i*	$As_{1.00}$	−0.0383(4)	0.1421(4)	0.1233(3)	0.0190(7)
S1	2*i*	$S_{1.00}$	−0.165(1)	0.7423(9)	0.3469(8)	0.028(2)
S2	2*i*	$S_{1.00}$	0.052(1)	0.1946(9)	0.3412(9)	0.032(2)
S3	2*i*	$S_{1.00}$	−0.1406(9)	0.3513(8)	0.1274(7)	0.016(2)
S4	2*i*	$S_{1.00}$	−0.344(1)	0.908(1)	0.1133(8)	0.030(2)
S5	2*i*	$S_{1.00}$	−0.570(1)	0.4765(9)	0.1487(9)	0.028(2)
S6	2*i*	$S_{1.00}$	0.219(1)	0.929(1)	0.1780(8)	0.024(2)
Te1	2*i*	$Te_{1.86(2)}S_{0.14}$	0.3521(3)	0.7157(3)	0.4993(2)	0.0258(8)

displacement parameters are reported in Table 2 (anisotropic atomic displacement parameters are listed in the accompanying CIF). Bond distances are given in Table 3. Calculated X-ray powder diffraction data, computed using the atom coordinates and occupancies reported in Table 2, are listed in Table 4. Structure factors and a crystallographic information file have been deposited with the Principal Editors of *Mineralogical Magazine* and are available at http://www.minersoc.org/pages/e_journals/dep_mat.html.

Chemical composition

A preliminary chemical analysis by energy-dispersive spectrometry was performed using a JEOL-5610 LV scanning electron microscope at the Museum of Natural History of Milan. The chemical composition was determined by wavelength-dispersive spectrometry (WDS) using a CAMECA-CAMEBAX electron microprobe. Major and minor elements were determined at 15 kV accelerating voltage and 15 nA beam

TABLE 3. Selected bond distances (Å) for debattistiite.

As1−S6	2.265(9)	As2−S5	2.249(8)	As3−S3	2.275(7)
−S1	2.289(8)	−S1	2.314(9)	−S4	2.317(9)
−S2	2.329(8)	−S4	2.327(8)	−S2	2.317(9)
<As1−S>	**2.294**	**<As2−S>**	**2.297**	**<As1−S>**	**2.303**
Ag1−S1	2.664(8)	Ag2−S4	2.662(9)	Ag3−S6	2.539(8)
−S3	2.670(8)	−Te1	2.853(4)	−S5	2.589(7)
−Te1	2.860(4)	−Te1	2.928(4)	−S3	2.671(7)
−Te1	2.950(4)				
<Ag1−S>	**2.786**	**<Ag2−S>**	**2.814**	**<Ag3−S>**	**2.600**
Ag4−S5	2.516(9)	Hg4−Te1	2.594(2)	Ag5−S6	2.560(8)
−S2	2.623(9)	−Te1	2.594(3)	−S3	2.571(7)
−Te1	2.916(5)	<Hg−Te>	2.594	−S5	2.675(8)
−Te1	2.947(5)				
<Ag4−S>	**2.751**	**<Hg−Te>**	**2.594**	**<Ag5−S>**	**2.6025**

TABLE 4. Calculated X-ray powder diffraction data for debattistiite.

I_{rel}	d_{calc}	h	k	l	I_{rel}	d_{calc}	h	k	l
62	10.5585	0	0	1	25	2.4800	1	1	3
10	7.5818	0	1	0	14	2.4576	$\bar{1}$	$\bar{1}$	4
15	6.9630	$\bar{1}$	1	0	11	2.3941	0	2	3
12	6.8961	1	0	0	14	2.3512	0	$\bar{2}$	4
6	6.2648	$\bar{1}$	0	1	15	2.2978	$\bar{2}$	1	4
6	5.3826	1	0	1	9	2.2421	3	$\bar{2}$	2
8	4.2634	$\bar{1}$	2	0	7	2.1159	$\bar{1}$	$\bar{3}$	1
5	4.1707	1	$\bar{1}$	2	6	2.1141	$\bar{2}$	3	3
14	3.5195	0	0	3	8	2.0926	$\bar{2}$	$\bar{1}$	4
8	3.4481	2	0	0	7	2.0521	1	$\bar{3}$	4
14	3.3980	0	2	1	20	1.9514	$\bar{4}$	2	1
14	3.3453	0	$\bar{2}$	2	6	1.9217	3	$\bar{3}$	3
47	3.3010	$\bar{2}$	1	2	26	1.9202	0	$\bar{4}$	1
7	3.2888	2	$\bar{2}$	1	5	1.9099	1	$\bar{4}$	3
15	3.1293	2	0	1	8	1.8981	$\bar{4}$	1	1
10	3.0263	1	1	2	6	1.8817	$\bar{4}$	3	1
11	3.0123	0	1	3	7	1.8583	$\bar{2}$	3	4
13	2.9972	$\bar{1}$	$\bar{1}$	3	8	1.8379	$\bar{2}$	$\bar{1}$	5
40	2.9906	2	$\bar{1}$	2	10	1.7598	0	0	6
10	2.9449	1	0	3	6	1.7588	$\bar{3}$	3	4
11	2.8680	0	2	2	5	1.7058	$\bar{1}$	4	3
18	2.8155	0	$\bar{2}$	3	5	1.6988	1	$\bar{1}$	6
95	2.7419	$\bar{2}$	$\bar{1}$	1	6	1.6505	$\bar{4}$	2	4
100	2.7329	$\bar{2}$	3	0	5	1.6444	4	$\bar{4}$	2
31	2.6396	0	0	4	5	1.6044	2	$\bar{5}$	3
6	2.6265	1	$\bar{3}$	2	8	1.5101	2	$\bar{3}$	6
10	2.6180	$\bar{2}$	3	1	8	0.7723	$\bar{5}$	$\bar{6}$	5
6	2.6140	$\bar{1}$	2	3	9	0.7710	$\bar{6}$	1	12
21	2.6129	$\bar{1}$	0	4	22	0.7710	$\bar{3}$	3	13
6	2.6016	1	2	1					

The calculated X-ray powder pattern was computed on the basis of a = 7.832(5), b = 8.606(4), c = 10.755(5) Å, α = 95.563(9), β = 95.880(5), γ = 116.79(4)°, and with the atomic coordinates and occupancies reported in Table 2. The five strongest lines are indicated in bold face.

current with a 1 μm beam diameter using 15 s counting times for both peaks and background. The X-ray lines used for the WDS analyses were as follows: S*K*α, Fe*K*α, Cu*K*α, Zn*K*α, As*L*α, Se*L*α, Te*L*α, Ag*L*α, Sb*L*β, Pb*M*α, Bi*M*β, and Hg*L*α. The elements Fe, Cu, Zn, Se, Sb, Pb and Bi were at or below the limit of detection of the electron microprobe (0.01 wt.%). The estimated analytical precision for the remaining elements is ±0.13 for Ag, ±0.09 for As, ±0.08 for S, ±0.06 for Te and ±0.04 for Hg. The standards employed were Ag metal for Ag, elemental Te for Te, synthetic As_2S_3 for As, cinnabar for Hg and pyrite for S. The crystal fragment was found to be homogeneous to within analytical error. The average chemical composition (nine analyses on different spots), and the wt.% ranges for the elements is reported in Table 5. On the basis of 29.5 atoms, the empirical formula for debattistiite is $Ag_{9.01}Hg_{0.49}As_{6.01}S_{11.98}Te_{2.01}$. The simplified ideal formula is $Ag_9Hg_{0.5}As_6S_{12}Te_2$, which requires: Ag 44.93, Hg 4.64, As 20.81, S 17.81, Te 11.81; total 100.00 wt.%.

Results and discussion

Description of the crystal structure

The crystal structure of debattistiite (Fig. 2) consists of three corner-sharing AsS_3 pyramids forming distorted rings that are linked by Ag polyhedra. A similar feature is present in the structure of trechmannite, $AgAsS_2$ (Matsumoto and Nowacki, 1969). In detail, Ag3 and Ag5 link three S atoms with mean bond distances of 2.600

TABLE 5. Electron-microprobe data (means and ranges in wt.% of elements on 9 analyses) with standard deviations (1σ) and analytical standards for debattistiite.

Element	Mean (wt.%)	Range	SD	Standard
Ag	44.88	44.43–45.26	0.13	Ag metal
Hg	4.49	4.11–4.68	0.04	cinnabar
As	20.77	20.21–21.30	0.09	synthetic As_2S_3
S	17.72	17.19–18.01	0.08	pyrite
Te	11.82	11.44–12.09	0.06	elemental Te
Total	99.68	98.96–100.68		

and 2.602 Å (Table 3). These values are in excellent agreement with those observed for silver atoms in triangular coordination in the structure of minerals of the pearceite–polybasite group (Bindi *et al.*, 2006, 2007; Evain *et al.*, 2006). The Ag2 links to one S and two Te/S atoms (i.e. the Te1 position) in a distorted triangular arrangement. The Ag1 and Ag4 sites have an interesting crystal-chemical environment, with a distorted tetrahedral coordination with 2 S and 2 Te/S atoms. These tetrahedra are strongly distorted with mean bond distances of 2.786 and 2.751 Å (Table 3). It is noteworthy that the two distances to S atoms are in keeping with those reported for tetrahedrally coordinated silver atoms in the structure of minerals of the pearceite–polybasite group (Bindi *et al.*, 2006, 2007; Evain *et al.*, 2006) and the two longest Te distances are similar to those reported in the hessite structure (2.8415(7)–3.034(1) Å; Van der Lee and de Boer, 1993).

The Hg atom is in a nearly perfect linear coordination with two Te/S atoms. The mean distance of 2.594 Å is greater than that in fettelite (<Hg–S> = 2.395 Å; Bindi *et al.*, 2009) and values reported in synthetic $[Hg\{S(CH_2)_2NH_3\}_2](Cl)_2$ (<Hg–S>: 2.333 and 2.338 Å; Kim *et al.*, 2002). This reflects the larger radius of Te in comparison to S. It is important to note that the Ag4 and the Hg positions (separation 1.137 Å) are partially occupied (50%). Thus there is a statistical distribution (50:50) between

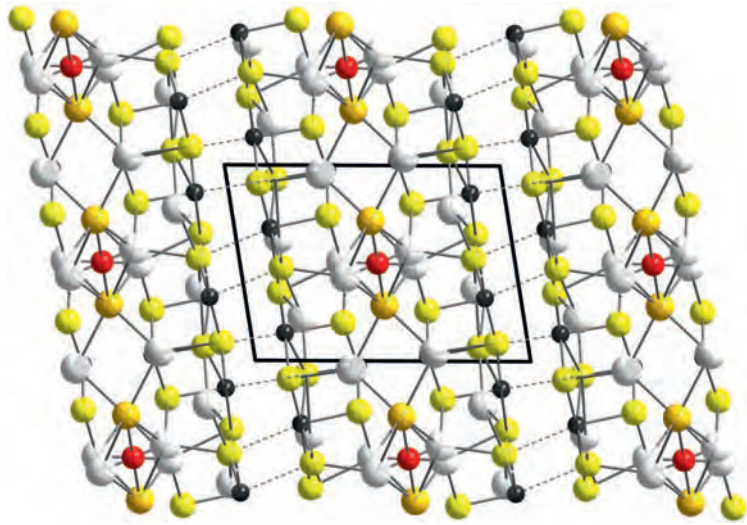

FIG. 2. The crystal structure of debattistiite projected down [100]. The Ag, Hg, As, S and Te atoms are indicated as white, red, black, yellow and orange spheres, respectively. The long As–S distances (lone pairs) are depicted using dashed lines. The unit cell is outlined.

$Hg(Te,S)_2$ and $AgS_2(Te,S)_2$ polyhedra in the structure (Fig. 3).

The Ag1–Ag1 and Ag4–Ag4 distances of 2.83 and 2.76 Å, respectively, are similar to those reported in face centred cubic silver (R_{Ag-Ag} = 2.89 Å; Suh *et al.*, 1988) and hexagonal close packed silver (R_{Ag-Ag} = 2.93 Å; Petruk *et al.*, 1970).

Possible origin and mineral association

Debattistiite is the second Te-bearing mineral to be found at Lengenbach after Te-bearing canfieldite (Bindi *et al.*, 2012). It occurs with trechmannite and hutchinsonite in dolomitic marble. In hydrothermal quartz veins, tellurium is found in tellurides such as muthmannite, krennerite, petzite and calaverite. The formation of sulfotellurides in hydrothermal systems indicates a relatively low fTe_2, insufficient for the formation of most S-free tellurides (Novoselov *et al.*, 2006). Estimates of the crystallization temperatures for sulfotellurides such as cervelleite, Ag_4TeS, have been proposed as >270ºC by Karup-Møller (1976) and 160–260ºC by Helmy (1999). Metastable sulfotellurides in association with native tellurium are thought to have formed at temperatures between 100 and 160ºC (Maslennikov, 1999). On the basis of their textural relationships and mineral associations it is thought that cervelleite and a sulfotelluride with the formula Ag_2Cu_2TeS formed at temperatures close to 400ºC in a skarn deposit (Cook and Ciobanu, 2003). These data show that estimating the temperature of formation is difficult for sulfotellurides due to the rarity or absence of thermodynamic data and the wide variety of geological environments in which they occur (Novoselov *et al.*, 2006). Recent work by Voudouris *et al.* (2011) indicates that sulfotellurides and cervelleite-like phases could have exsolved from galena during cooling below 200ºC. These authors suggest that the initial temperatures for the formation of sulfotellurides could be close to 300ºC. Oberthür and Weiser (2008) studied an assemblage of Au-Bi-Te-S minerals (joseite-A, joseite-B and hessite) and proposed that such an assemblage can form in reducing conditions at relatively low fS_2 and fTe_2 at temperatures of ~340ºC.

The Lengenbach mineralization is in a Triassic dolostone marble which formed during greenschist to lower amphibolite facies Alpine metamorphism in the temperature range 400–500ºC. Metamorphic processes remobilized the primary mineralization, which was originally a stratiform carbonate-hosted orebody (Vokes, 1971; Hofmann and Knill, 1996). Cooling of sulfide melts led to the formation of massive to well-crystallized sulfides and sulfosalts from aqueous hydrothermal fluids at estimated temperatures >330ºC (Hofmann, 1994). It is therefore suggested that debattistiite formed from hydrothermal solutions at similar temperatures to those reported for the other Lengenbach sulfosalts.

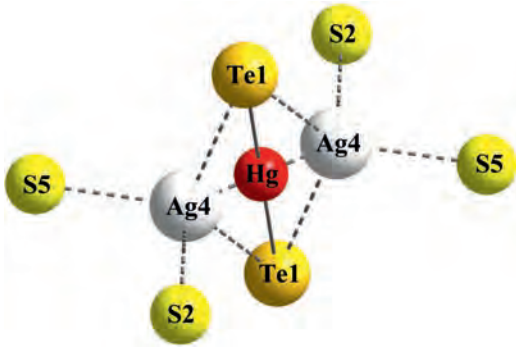

FIG. 3. The crystal-chemical environment of the Ag4 site and Hg atoms. The Ag, Hg, S and Te atoms are indicated as white, red, yellow and orange spheres, respectively. The Ag4 site and Hg are very close (separation 1.137 Å), so there is a statistical distribution (50:50) between $Hg(Te,S)_2$ and $AgS_2(Te,S)_2$ polyhedra in the structure. The Hg–(Te,S) distances are indicated using solid lines whereas the Ag–S and the Ag–(Te,S) distances are indicated using dashed lines.

Acknowledgements

The research was supported by a grant from the "progetto d'Ateneo 2006, University of Padova" to FN. We thank Federico Pezzotta of Natural History Museum of Milan for the preliminary analyses by SEM and Michele Zilioli for his useful contribution in obtaining SEM images. The two referees S. Mills and F. Laufek are thanked for their helpful revisions.

References

Bindi, L., Evain, M. and Menchetti, S. (2006) Temperature dependence of the silver distribution in the crystal structure of natural pearceite, $(Ag,Cu)_{16}(As,Sb)_2S_{11}$. *Acta Crystallographica*, **B62**, 212–219.

Bindi, L., Evain, M. and Menchetti, S. (2007) Complex twinning, polytypism and disorder phenomena in the

crystal structures of antimonpearceite and arsenpolybasite. *The Canadian Mineralogist*, **45**, 321–333.

Bindi, L., Keutsch, F.N., Francis, C.A. and Menchetti, S. (2009) Fettelite, $[Ag_6As_2S_7][Ag_{10}HgAs_2S_8]$ from Chañarcillo, Chile: crystal structure, pseudosymmetry, twinning, and revised chemical formula. *American Mineralogist*, **94**, 609–615.

Bindi, L., Nestola, F., Guastoni, A. and Secco, L. (2011) The crustal structure of dalnegroite, $Tl_{5-x}Pb_{2x}(As,Sb)_{21-x}S_{34}$: a masterpiece of structural complexity. *Mineralogical Magazine*, **74**, 999–1012.

Bindi, L., Nestola, F., Guastoni, A., Zorzi, F., Peruzzo, L. and Raber T. (2012) Tellurian canfieldite, AgSn(S,Te), from Lengenbach quarry, Binntal, Canton Valais, Switzerland: occurrence, description and crustal structure. *The Canadian Mineralogist*, http://dx.doi.org/10.3749/canmin.50.1.000.

Cook, N.J. and Ciobanu, C.L. (2003) Cervelleite, Ag_4TeS, from three localities in Romania, substitution of Cu, and the occurrence of the associated phase Ag_2Cu_2TeS. *Neues Jahrbuch für Mineralogie, Monatshefte*, **2003**, 321–336.

Evain, M., Bindi, L. and Menchetti, S. (2006) Structural complexity in minerals: twinning, polytypism and disorder in the crystal structure of polybasite, $(Ag,Cu)_{16}(Sb,As)_2S_{11}$. *Acta Crystallographica*, **B62**, 447–456.

Graeser, S., Cannon, R., Drechsler, E., Raber, T. and Roth, P. (2008) *Faszination Lengenbach Abbau-Forschung-Mineralien 1958–2008*. Kristallographik Verlag, Achberg, Germany.

Guastoni, A. and De Battisti, L. (2006) Thalcusite. Un altro minerale di tallio scoperto a Lengenbach, Valle di Binn, Svizzera. *Rivista Mineralogica Italiana*, **30**, 54–55.

Helmy, H. (1999) The Um Samiuki volcanogenic Zn–Cu–Pb–Ag deposit, Eastern Desert, Egypt: a possible new occurrence of cervelleite. *The Canadian Mineralogist*, **37**, 143–158.

Hofmann, B. (1994) Formation of a sulfide melt during Alpine metamorphism of the Lengenbach polymetallic sulfide mineralization, Binntal, Switzerland. *Mineralium Deposita*, **29**, 439–442.

Hofmann, B. and Knill, M.D. (1996) Geochemistry and genesis of the Lengenbach Pb-Zn-As-Tl-Ba mineralisation, Binn Valley, Switzerland. *Mineralium Deposita*, **31**, 319–339.

Hofmann, B., Graeser, S., Imhof, T., Sicher, V. and Stalder, H.A. (1993) Mineralogie der Grube Lengenbach, Binntal, Wallis. Zum 35-jährigen Bestehen der Arbeitsgemeinshaft Lengenbach. *Jahrbuch Naturhistorische Museum der Bern*, **11**, 3–90.

Ibers, J.A. and Hamilton, W.C. (editors) (1974) *International Tables for X-ray Crystallography*, volume IV. Kynock Press, Birmingham, UK, 366 pp.

Karup-Møller, S. (1976) Arcubisite and mineral B – two new minerals from the cryolite deposit at Ivigtut, South Greenland. *Lithos*, **4**, 253–257.

Kim, C.-H., Parkin, S., Bharara, M. and Atwood, D. (2002) Linear coordination of Hg(II) by cysteamine. *Polyhedron*, **21**, 225–228.

Maslennikov, V.V. (1999) *Sedimentogenesis, Halmyrolysis and Ecology of Massive Sulphide Bearing Paleohydrothermal Fields (after example of the South Urals)*. Geotur, Miass, Russia, 348 pp, [in Russian].

Matsumoto, T. and Nowacki, W. (1969) The crystal structure of trechmannite, $AgAsS_2$. *Zeitschrift für Kristallographie*, **129**, 163–177.

Nestola, F., Guastoni, A., Bindi, L. and Secco L. (2010) Dalnegroite, $Tl_{5-x}Pb_{2x}(As,Sb)_{21-x}S_{34}$, a new thallium sulphosalt from Lengenbach quarry, Binntal, Canton Valais, Switzerland. *Mineralogical Magazine*, **73**, 1027–1032.

Novoselov, K.A., Belogub, E.V., Zaykov, V.V. and Yakovleva V.A. (2006) Silver sulfotellurides from volcanic-hosted massive sulfide deposits in the Southern Urals. *Mineralogy and Petrology*, **87**, 327–349.

Oberthür, T. and Weiser, T.W. (2008) Gold-bismuth-telluride-sulphide assemblages at the Viceroy Mine, Harare-Bindura-Shamva greenstone belt, Zimbabwe. *Mineralogical Magazine*, **72**, 953–970.

Oszlányi, G. and Süto, A. (2008) The charge flipping algorithm. *Acta Crstallographica*, **A64**, 123–134.

Petříček, V., Dusek, M. and Palatinus, L. (2006) *JANA2006, Structure Determination Software Programs*. Institute of Physics, Academy of Sciences of the Czech Republic, Prague, Czech Republic.

Petruk, W., Cabri, L.J., Harris, D.C., Stewart, J.M. and Clark, L.A. (1970) Allargentum, redefined. *The Canadian Mineralogist*, **10**, 163–172.

Suh, I.-K., Ohta, H. and Waseda, Y. (1988) High-temperature thermal expansion of six metallic elements measured by dilatation method and X-ray diffraction. *Journal of Materials Science*, **23**, 757–760.

Van der Lee, A. and de Boer, J.L. (1993) Redetermination of the structure of hessite, Ag_2Te-III. *Acta Crystallographica*, **C49**, 1444–1446.

Vokes, F.M. (1971) Some aspects of the regional metamorphic mobilization of preexisting sulphide deposits. *Mineralium Deposita*, **6**, 122–129.

Voudouris P.C., Spry, P.G., Sakellaris, G.A. and Mavrogonatos, C. (2011) A cervelleite-like mineral and other Ag-Cu-Te-S minerals [Ag_2CuTeS and $(Ag,Cu)_2TeS$] in gold-bearing veins in metamorphic rocks of the Cycladic Blueschist Unit, Kallianou, Evia Island, Greece. *Mineralogy and Petrology*, **101**, 169–183.

```
data_luca

_audit_creation_method            SHELXL-97
_chemical_name_systematic
;
 ?
;
_chemical_name_common             ?
_chemical_melting_point           ?
_chemical_formula_moiety          ?
_chemical_formula_sum
 'Ag16 As6 Hg0 S12 Te2'
_chemical_formula_weight          2815.36

loop_
 _atom_type_symbol
 _atom_type_description
 _atom_type_scat_dispersion_real
 _atom_type_scat_dispersion_imag
 _atom_type_scat_source
 'Ag'  'Ag'  -0.8971   1.1015
 'International Tables Vol C Tables 4.2.6.8 and 6.1.1.4'
 'As'  'As'   0.0499   2.0058
 'International Tables Vol C Tables 4.2.6.8 and 6.1.1.4'
 'S'  'S'   0.1246   0.1234
 'International Tables Vol C Tables 4.2.6.8 and 6.1.1.4'
 'Te'  'Te'  -0.5308   1.6751
 'International Tables Vol C Tables 4.2.6.8 and 6.1.1.4'
 'Hg'  'Hg'  -2.3894   9.2266
 'International Tables Vol C Tables 4.2.6.8 and 6.1.1.4'

_symmetry_cell_setting            ?
_symmetry_space_group_name_H-M    ?

loop_
 _symmetry_equiv_pos_as_xyz
 'x, y, z'
 '-x, -y, -z'

_cell_length_a                    7.832(5)
_cell_length_b                    8.606(4)
_cell_length_c                    10.755(5)
_cell_angle_alpha                 95.563(9)
_cell_angle_beta                  95.880(5)
_cell_angle_gamma                 116.79(4)
_cell_volume                      635.3(6)
_cell_formula_units_Z             1
_cell_measurement_temperature     293(2)
_cell_measurement_reflns_used     ?
_cell_measurement_theta_min       ?
_cell_measurement_theta_max       ?

_exptl_crystal_description        ?
_exptl_crystal_colour             ?
_exptl_crystal_size_max           ?
_exptl_crystal_size_mid           ?
_exptl_crystal_size_min           ?
_exptl_crystal_density_meas       ?
_exptl_crystal_density_diffrn     7.359
```

```
_exptl_crystal_density_method     'not measured'
_exptl_crystal_F_000              1246
_exptl_absorpt_coefficient_mu     23.011
_exptl_absorpt_correction_type    ?
_exptl_absorpt_correction_T_min   ?
_exptl_absorpt_correction_T_max   ?
_exptl_absorpt_process_details    ?

_exptl_special_details
;
 ?
;

_diffrn_ambient_temperature       293(2)
_diffrn_radiation_wavelength      0.71073
_diffrn_radiation_type            MoK\a
_diffrn_radiation_source          'fine-focus sealed tube'
_diffrn_radiation_monochromator   graphite
_diffrn_measurement_device_type   ?
_diffrn_measurement_method        ?
_diffrn_detector_area_resol_mean  ?
_diffrn_standards_number          ?
_diffrn_standards_interval_count  ?
_diffrn_standards_interval_time   ?
_diffrn_standards_decay_%         ?
_diffrn_reflns_number             8404
_diffrn_reflns_av_R_equivalents   0.1247
_diffrn_reflns_av_sigmaI/netI     0.7900
_diffrn_reflns_limit_h_min        -12
_diffrn_reflns_limit_h_max        12
_diffrn_reflns_limit_k_min        -7
_diffrn_reflns_limit_k_max        16
_diffrn_reflns_limit_l_min        -16
_diffrn_reflns_limit_l_max        20
_diffrn_reflns_theta_min          2.93
_diffrn_reflns_theta_max          43.09
_reflns_number_total              5635
_reflns_number_gt                 795
_reflns_threshold_expression      >2sigma(I)

_computing_data_collection        ?
_computing_cell_refinement        ?
_computing_data_reduction         ?
_computing_structure_solution     ?
_computing_structure_refinement   'SHELXL-97 (Sheldrick, 1997)'
_computing_molecular_graphics     ?
_computing_publication_material   ?

_refine_special_details
;
 Refinement of F^2^ against ALL reflections.  The weighted R-factor wR and
 goodness of fit S are based on F^2^, conventional R-factors R are based
 on F, with F set to zero for negative F^2^. The threshold expression of
 F^2^ > 2sigma(F^2^) is used only for calculating R-factors(gt) etc. and is
 not relevant to the choice of reflections for refinement.  R-factors based
 on F^2^ are statistically about twice as large as those based on F, and R-
 factors based on ALL data will be even larger.
;

_refine_ls_structure_factor_coef  Fsqd
_refine_ls_matrix_type            full
```

```
_refine_ls_weighting_scheme       calc
_refine_ls_weighting_details
 'calc w=1/[\s^2^(Fo^2^)+(0.0418P)^2^+0.0000P] where P=(Fo^2^+2Fc^2^)/3'
_atom_sites_solution_primary      direct
_atom_sites_solution_secondary    difmap
_atom_sites_solution_hydrogens    geom
_refine_ls_hydrogen_treatment     mixed
_refine_ls_extinction_method      none
_refine_ls_extinction_coef        ?
_refine_ls_number_reflns          5635
_refine_ls_number_parameters      133
_refine_ls_number_restraints      0
_refine_ls_R_factor_all           0.1012
_refine_ls_R_factor_gt            0.0826
_refine_ls_wR_factor_ref          0.2104
_refine_ls_wR_factor_gt           0.1733
_refine_ls_goodness_of_fit_ref    0.700
_refine_ls_restrained_S_all       0.700
_refine_ls_shift/su_max           0.009
_refine_ls_shift/su_mean          0.001

loop_
 _atom_site_label
 _atom_site_type_symbol
 _atom_site_fract_x
 _atom_site_fract_y
 _atom_site_fract_z
 _atom_site_U_iso_or_equiv
 _atom_site_adp_type
 _atom_site_occupancy
 _atom_site_symmetry_multiplicity
 _atom_site_calc_flag
 _atom_site_refinement_flags
 _atom_site_disorder_assembly
 _atom_site_disorder_group
Ag1 Ag -0.0372(4) 0.5057(3) 0.3695(3) 0.0453(9) Uani 1 1 d . . .
Ag2 Ag 0.5761(4) 0.9562(4) 0.3442(3) 0.0600(10) Uani 1 1 d . . .
Ag3 Ag 0.2110(4) 0.6290(3) 0.1574(4) 0.0665(12) Uani 1 1 d . . .
Hg4 Hg 0.5000 0.5000 0.5000 0.0240(16) Uiso 0.50 2 d SP . .
Ag4 Ag 0.5814(6) 0.5688(5) 0.6241(4) 0.0192(10) Uiso 0.50 1 d P . .
Ag5 Ag 0.5248(4) 0.2238(4) 1.1972(4) 0.0787(14) Uani 1 1 d . . .
As1 As 0.1403(4) 0.9740(4) 0.3703(3) 0.0205(8) Uani 1 1 d . . .
As2 As -0.2694(4) 0.6768(4) 0.1302(3) 0.0237(8) Uani 1 1 d . . .
As3 As -0.0383(4) 1.1421(4) 0.1233(3) 0.0190(7) Uani 1 1 d . . .
S1 S -0.1650(10) 0.7423(9) 0.3469(8) 0.028(2) Uani 1 1 d . . .
S2 S 0.0524(11) 1.1946(9) 0.3412(9) 0.032(2) Uani 1 1 d . . .
S3 S -0.1406(9) 0.3513(8) 0.1274(7) 0.0161(16) Uani 1 1 d . . .
S4 S -0.3441(11) 0.9075(10) 0.1133(8) 0.030(2) Uani 1 1 d . . .
S5 S -0.5701(10) 0.4765(9) 0.1487(9) 0.028(2) Uani 1 1 d . . .
S6 S 0.2186(10) 0.9285(10) 0.1780(8) 0.0238(18) Uani 1 1 d . . .
Te1 Te 0.3521(3) 0.7157(3) 0.4993(2) 0.0258(8) Uani 0.942(10) 1 d P . .
SE1 S 0.3521(3) 0.7157(3) 0.4993(2) 0.0258(8) Uani 0.058(10) 1 d P . .

loop_
 _atom_site_aniso_label
 _atom_site_aniso_U_11
 _atom_site_aniso_U_22
 _atom_site_aniso_U_33
 _atom_site_aniso_U_23
 _atom_site_aniso_U_13
 _atom_site_aniso_U_12
```

```
Ag1 0.0385(17) 0.0421(17) 0.061(2) 0.0058(15) 0.0020(15) 0.0253(15)
Ag2 0.060(2) 0.066(2) 0.077(3) 0.0210(19) 0.0385(18) 0.0421(19)
Ag3 0.0380(18) 0.0290(16) 0.146(4) 0.0166(19) 0.039(2) 0.0221(15)
Ag5 0.0334(18) 0.048(2) 0.174(4) 0.040(2) 0.046(2) 0.0255(16)
As1 0.0165(16) 0.0228(17) 0.027(2) 0.0048(14) 0.0038(14) 0.0135(14)
As2 0.0103(15) 0.0104(15) 0.052(3) 0.0120(15) 0.0102(15) 0.0043(13)
As3 0.0137(15) 0.0127(15) 0.033(2) 0.0066(14) 0.0077(14) 0.0069(13)
S1 0.018(4) 0.014(4) 0.049(6) 0.007(4) 0.007(4) 0.004(3)
S2 0.024(4) 0.014(4) 0.059(7) 0.006(4) 0.012(4) 0.008(4)
S3 0.007(3) 0.004(3) 0.033(5) 0.007(3) -0.002(3) -0.001(3)
S4 0.022(4) 0.029(5) 0.046(6) 0.002(4) -0.001(4) 0.020(4)
S5 0.015(4) 0.016(4) 0.057(6) 0.011(4) 0.008(4) 0.009(3)
S6 0.015(4) 0.033(5) 0.026(5) 0.008(4) 0.000(3) 0.013(4)
Te1 0.0217(13) 0.0238(13) 0.0366(16) 0.0079(10) 0.0062(10) 0.0137(10)
SE1 0.0217(13) 0.0238(13) 0.0366(16) 0.0079(10) 0.0062(10) 0.0137(10)

_geom_special_details
;
 All esds (except the esd in the dihedral angle between two l.s. planes)
 are estimated using the full covariance matrix.  The cell esds are taken
 into account individually in the estimation of esds in distances, angles
 and torsion angles; correlations between esds in cell parameters are only
 used when they are defined by crystal symmetry.  An approximate (isotropic)
 treatment of cell esds is used for estimating esds involving l.s. planes.
;

loop_
 _geom_bond_atom_site_label_1
 _geom_bond_atom_site_label_2
 _geom_bond_distance
 _geom_bond_site_symmetry_2
 _geom_bond_publ_flag
Ag1 S1 2.664(8) . ?
Ag1 S3 2.670(8) . ?
Ag1 Ag1 2.827(6) 2_566 ?
Ag1 Te1 2.860(4) . ?
Ag1 SE1 2.950(4) 2_566 ?
Ag1 Te1 2.950(4) 2_566 ?
Ag1 Ag3 3.103(5) . ?
Ag1 Ag5 3.378(5) 1_454 ?
Ag2 S4 2.662(9) 1_655 ?
Ag2 Te1 2.853(4) . ?
Ag2 SE1 2.928(4) 2_676 ?
Ag2 Te1 2.928(4) 2_676 ?
Ag2 Ag5 3.061(5) 1_564 ?
Ag2 Ag3 3.257(5) . ?
Ag3 S6 2.539(8) . ?
Ag3 S5 2.589(7) 1_655 ?
Ag3 S3 2.671(7) . ?
Hg4 Ag4 1.367(4) . ?
Hg4 Ag4 1.367(4) 2_666 ?
Hg4 Te1 2.594(2) . ?
Hg4 SE1 2.594(2) 2_666 ?
Hg4 Te1 2.594(2) 2_666 ?
Ag4 S5 2.516(10) 2_566 ?
Ag4 S2 2.623(9) 2_676 ?
Ag4 Ag4 2.735(9) 2_666 ?
Ag4 Ag5 2.928(5) 2_667 ?
Ag4 Te1 2.916(5) . ?
Ag4 SE1 2.947(5) 2_666 ?
Ag4 Te1 2.947(5) 2_666 ?
```

```
Ag5 S6 2.560(8) 1_546 ?
Ag5 S3 2.571(7) 1_656 ?
Ag5 S5 2.675(8) 1_656 ?
Ag5 Ag4 2.928(5) 2_667 ?
Ag5 Ag2 3.061(5) 1_546 ?
Ag5 Te1 3.230(5) 2_667 ?
Ag5 Ag1 3.378(5) 1_656 ?
As1 S6 2.265(9) . ?
As1 S1 2.289(8) . ?
As1 S2 2.329(8) . ?
As2 S5 2.249(8) . ?
As2 S4 2.327(8) . ?
As2 S1 2.314(9) . ?
As3 S3 2.275(7) 1_565 ?
As3 S4 2.317(9) . ?
As3 S2 2.317(10) . ?
S2 Ag4 2.623(9) 2_676 ?
S3 As3 2.275(7) 1_545 ?
S3 Ag5 2.571(7) 1_454 ?
S4 Ag2 2.662(9) 1_455 ?
S5 Ag4 2.516(10) 2_566 ?
S5 Ag3 2.589(7) 1_455 ?
S5 Ag5 2.675(8) 1_454 ?
S6 Ag5 2.560(8) 1_564 ?
Te1 Ag2 2.928(4) 2_676 ?
Te1 Ag1 2.950(4) 2_566 ?
Te1 Ag4 2.947(5) 2_666 ?
Te1 Ag5 3.230(5) 2_667 ?

loop_
 _geom_angle_atom_site_label_1
 _geom_angle_atom_site_label_2
 _geom_angle_atom_site_label_3
 _geom_angle
 _geom_angle_site_symmetry_1
 _geom_angle_site_symmetry_3
 _geom_angle_publ_flag
S1 Ag1 S3 97.4(2) . . ?
S1 Ag1 Ag1 107.8(2) . 2_566 ?
S3 Ag1 Ag1 151.2(2) . 2_566 ?
S1 Ag1 Te1 102.95(19) . . ?
S3 Ag1 Te1 125.66(18) . . ?
Ag1 Ag1 Te1 62.48(11) 2_566 . ?
S1 Ag1 SE1 94.3(2) . 2_566 ?
S3 Ag1 SE1 105.91(17) . 2_566 ?
Ag1 Ag1 SE1 59.31(12) 2_566 2_566 ?
Te1 Ag1 SE1 121.79(12) . 2_566 ?
S1 Ag1 Te1 94.3(2) . 2_566 ?
S3 Ag1 Te1 105.91(17) . 2_566 ?
Ag1 Ag1 Te1 59.31(12) 2_566 2_566 ?
Te1 Ag1 Te1 121.79(12) . 2_566 ?
SE1 Ag1 Te1 0.00(14) 2_566 2_566 ?
S1 Ag1 Ag3 91.7(2) . . ?
S3 Ag1 Ag3 54.49(17) . . ?
Ag1 Ag1 Ag3 135.89(16) 2_566 . ?
Te1 Ag1 Ag3 74.91(11) . . ?
SE1 Ag1 Ag3 160.16(12) 2_566 . ?
Te1 Ag1 Ag3 160.16(12) 2_566 . ?
S1 Ag1 Ag5 83.41(18) . 1_454 ?
S3 Ag1 Ag5 48.58(16) . 1_454 ?
Ag1 Ag1 Ag5 119.74(16) 2_566 1_454 ?
```

```
Te1 Ag1 Ag5 172.48(12) . 1_454 ?
SE1 Ag1 Ag5 60.93(10) 2_566 1_454 ?
Te1 Ag1 Ag5 60.93(10) 2_566 1_454 ?
Ag3 Ag1 Ag5 101.15(13) . 1_454 ?
S4 Ag2 Te1 132.2(2) 1_655 . ?
S4 Ag2 SE1 129.1(2) 1_655 2_676 ?
Te1 Ag2 SE1 98.10(11) . 2_676 ?
S4 Ag2 Te1 129.1(2) 1_655 2_676 ?
Te1 Ag2 Te1 98.10(11) . 2_676 ?
SE1 Ag2 Te1 0.00(11) 2_676 2_676 ?
S4 Ag2 Ag5 72.33(19) 1_655 1_564 ?
Te1 Ag2 Ag5 134.82(13) . 1_564 ?
SE1 Ag2 Ag5 65.21(11) 2_676 1_564 ?
Te1 Ag2 Ag5 65.21(11) 2_676 1_564 ?
S4 Ag2 Ag3 67.8(2) 1_655 . ?
Te1 Ag2 Ag3 72.59(11) . . ?
SE1 Ag2 Ag3 136.95(12) 2_676 . ?
Te1 Ag2 Ag3 136.95(12) 2_676 . ?
Ag5 Ag2 Ag3 91.33(14) 1_564 . ?
S6 Ag3 S5 142.9(3) . 1_655 ?
S6 Ag3 S3 115.6(2) . . ?
S5 Ag3 S3 101.4(2) 1_655 . ?
S6 Ag3 Ag1 94.2(2) . . ?
S5 Ag3 Ag1 109.0(2) 1_655 . ?
S3 Ag3 Ag1 54.47(18) . . ?
S6 Ag3 Ag2 62.35(18) . . ?
S5 Ag3 Ag2 86.7(2) 1_655 . ?
S3 Ag3 Ag2 149.1(2) . . ?
Ag1 Ag3 Ag2 94.61(13) . . ?
Ag4 Hg4 Ag4 180.000(1) . 2_666 ?
Ag4 Hg4 Te1 89.26(18) . . ?
Ag4 Hg4 Te1 90.74(18) 2_666 . ?
Ag4 Hg4 SE1 90.74(18) . 2_666 ?
Ag4 Hg4 SE1 89.26(18) 2_666 2_666 ?
Te1 Hg4 SE1 180.000(1) . 2_666 ?
Ag4 Hg4 Te1 90.74(18) . 2_666 ?
Ag4 Hg4 Te1 89.26(18) 2_666 2_666 ?
Te1 Hg4 Te1 180.000(1) . 2_666 ?
SE1 Hg4 Te1 0.00(11) 2_666 2_666 ?
Hg4 Ag4 S5 146.6(3) . 2_566 ?
Hg4 Ag4 S2 114.4(3) . 2_676 ?
S5 Ag4 S2 96.4(3) 2_566 2_676 ?
Hg4 Ag4 Ag4 0.00(9) . 2_666 ?
S5 Ag4 Ag4 146.6(3) 2_566 2_666 ?
S2 Ag4 Ag4 114.4(3) 2_676 2_666 ?
Hg4 Ag4 Ag5 127.7(2) . 2_667 ?
S5 Ag4 Ag5 58.27(19) 2_566 2_667 ?
S2 Ag4 Ag5 94.1(2) 2_676 2_667 ?
Ag4 Ag4 Ag5 127.7(2) 2_666 2_667 ?
Hg4 Ag4 Te1 62.78(16) . . ?
S5 Ag4 Te1 121.1(2) 2_566 . ?
S2 Ag4 Te1 108.2(2) 2_676 . ?
Ag4 Ag4 Te1 62.78(16) 2_666 . ?
Ag5 Ag4 Te1 67.09(13) 2_667 . ?
Hg4 Ag4 SE1 61.63(16) . 2_666 ?
S5 Ag4 SE1 105.2(2) 2_566 2_666 ?
S2 Ag4 SE1 94.3(2) 2_676 2_666 ?
Ag4 Ag4 SE1 61.63(16) 2_666 2_666 ?
Ag5 Ag4 SE1 162.27(18) 2_667 2_666 ?
Te1 Ag4 SE1 124.41(16) . 2_666 ?
Hg4 Ag4 Te1 61.63(16) . 2_666 ?
```

S5 Ag4 Te1 105.2(2) 2_566 2_666 ?
S2 Ag4 Te1 94.3(2) 2_676 2_666 ?
Ag4 Ag4 Te1 61.63(16) 2_666 2_666 ?
Ag5 Ag4 Te1 162.27(18) 2_667 2_666 ?
Te1 Ag4 Te1 124.41(16) . 2_666 ?
SE1 Ag4 Te1 0.00(4) 2_666 2_666 ?
S6 Ag5 S3 139.8(3) 1_546 1_656 ?
S6 Ag5 S5 110.2(3) 1_546 1_656 ?
S3 Ag5 S5 99.0(2) 1_656 1_656 ?
S6 Ag5 Ag4 97.7(2) 1_546 2_667 ?
S3 Ag5 Ag4 122.2(2) 1_656 2_667 ?
S5 Ag5 Ag4 53.1(2) 1_656 2_667 ?
S6 Ag5 Ag2 65.33(19) 1_546 1_546 ?
S3 Ag5 Ag2 96.34(18) 1_656 1_546 ?
S5 Ag5 Ag2 158.3(2) 1_656 1_546 ?
Ag4 Ag5 Ag2 105.40(17) 2_667 1_546 ?
S6 Ag5 Te1 97.0(2) 1_546 2_667 ?
S3 Ag5 Te1 100.8(2) 1_656 2_667 ?
S5 Ag5 Te1 106.3(2) 1_656 2_667 ?
Ag4 Ag5 Te1 56.28(12) 2_667 2_667 ?
Ag2 Ag5 Te1 55.41(10) 1_546 2_667 ?
S6 Ag5 Ag1 146.2(2) 1_546 1_656 ?
S3 Ag5 Ag1 51.17(18) 1_656 1_656 ?
S5 Ag5 Ag1 94.7(2) 1_656 1_656 ?
Ag4 Ag5 Ag1 78.93(14) 2_667 1_656 ?
Ag2 Ag5 Ag1 83.03(13) 1_546 1_656 ?
Te1 Ag5 Ag1 52.96(9) 2_667 1_656 ?
S6 As1 S1 100.4(3) . . ?
S6 As1 S2 100.1(3) . . ?
S1 As1 S2 98.0(3) . . ?
S5 As2 S4 95.8(3) . . ?
S5 As2 S1 93.1(3) . . ?
S4 As2 S1 96.9(3) . . ?
S3 As3 S4 95.2(3) 1_565 . ?
S3 As3 S2 93.1(3) 1_565 . ?
S4 As3 S2 97.3(3) . . ?
As1 S1 As2 103.9(3) . . ?
As1 S1 Ag1 93.7(3) . . ?
As2 S1 Ag1 98.6(3) . . ?
As1 S2 As3 101.3(3) . . ?
As1 S2 Ag4 90.6(3) . 2_676 ?
As3 S2 Ag4 103.3(3) . 2_676 ?
As3 S3 Ag5 108.3(3) 1_545 1_454 ?
As3 S3 Ag3 96.5(2) 1_545 . ?
Ag5 S3 Ag3 145.8(3) 1_454 . ?
As3 S3 Ag1 103.6(3) 1_545 . ?
Ag5 S3 Ag1 80.2(2) 1_454 . ?
Ag3 S3 Ag1 71.05(19) . . ?
As3 S4 As2 101.2(3) . . ?
As3 S4 Ag2 102.7(3) . 1_455 ?
As2 S4 Ag2 100.1(3) . 1_455 ?
As2 S5 Ag4 109.5(3) . 2_566 ?
As2 S5 Ag3 109.1(3) . 1_455 ?
Ag4 S5 Ag3 92.3(3) 2_566 1_455 ?
As2 S5 Ag5 95.8(3) . 1_454 ?
Ag4 S5 Ag5 68.6(2) 2_566 1_454 ?
Ag3 S5 Ag5 152.8(3) 1_455 1_454 ?
As1 S6 Ag3 106.3(3) . . ?
As1 S6 Ag5 97.7(3) . 1_564 ?
Ag3 S6 Ag5 124.9(3) . 1_564 ?
Hg4 Te1 Ag2 102.02(10) . . ?

```
Hg4 Te1 Ag1 104.65(10) . . ?
Ag2 Te1 Ag1 109.86(13) . . ?
Hg4 Te1 Ag2 136.17(11) . 2_676 ?
Ag2 Te1 Ag2 81.90(11) . 2_676 ?
Ag1 Te1 Ag2 115.04(11) . 2_676 ?
Hg4 Te1 Ag4 27.96(9) . . ?
Ag2 Te1 Ag4 109.57(13) . . ?
Ag1 Te1 Ag4 123.45(13) . . ?
Ag2 Te1 Ag4 109.23(14) 2_676 . ?
Hg4 Te1 Ag1 92.17(9) . 2_566 ?
Ag2 Te1 Ag1 163.82(11) . 2_566 ?
Ag1 Te1 Ag1 58.21(12) . 2_566 ?
Ag2 Te1 Ag1 93.32(11) 2_676 2_566 ?
Ag4 Te1 Ag1 86.61(12) . 2_566 ?
Hg4 Te1 Ag4 27.64(9) . 2_666 ?
Ag2 Te1 Ag4 92.00(13) . 2_666 ?
Ag1 Te1 Ag4 84.25(12) . 2_666 ?
Ag2 Te1 Ag4 160.70(13) 2_676 2_666 ?
Ag4 Te1 Ag4 55.59(16) . 2_666 ?
Ag1 Te1 Ag4 97.18(12) 2_566 2_666 ?
Hg4 Te1 Ag5 83.77(8) . 2_667 ?
Ag2 Te1 Ag5 122.70(12) . 2_667 ?
Ag1 Te1 Ag5 123.78(11) . 2_667 ?
Ag2 Te1 Ag5 59.38(10) 2_676 2_667 ?
Ag4 Te1 Ag5 56.63(11) . 2_667 ?
Ag1 Te1 Ag5 66.11(10) 2_566 2_667 ?
Ag4 Te1 Ag5 110.69(12) 2_666 2_667 ?

_diffrn_measured_fraction_theta_max    0.596
_diffrn_reflns_theta_full              43.09
_diffrn_measured_fraction_theta_full   0.596
_refine_diff_density_max    3.049
_refine_diff_density_min   -4.986
_refine_diff_density_rms    0.575
```